Received: 2 December 2021 | Revised: 19 January 2022 | Accepted: 15 March 2022

DOI: 10.4218/etrij.2021-0456

ORIGINAL ARTICLE

ETRI Journal WILEY

# Least squares decoding in binomial frequency division multiplexing

**Myungsup Kim** | **Jiwon Jung** | **Ki-Man Kim**

Department of Radio Communications, Korea Maritime and Ocean University, Busan, Republic of Korea

**Correspondence**
Jiwon Jung, Department of Radio Communications, Korea Maritime and Ocean University, Busan, Republic of Korea.
Email: jwjung@kmou.ac.kr

**Abstract**

This paper proposes a method that can reduce the complexity of a system matrix by analyzing the characteristics of a pseudoinverse matrix to receive a binomial frequency division multiplexing (BFDM) signal and decode it using the least squares (LS) method. The system matrix of BFDM can be expressed as a band matrix, and as this matrix contains many zeros, its amount of calculation when generating a transmission signal is quite small. The LS solution can be obtained by multiplying the received signal by the pseudoinverse matrix of the system matrix. The singular value decomposition of the system matrix indicates that the pseudoinverse matrix is a band matrix. The signal-to-interference ratio is obtained from their eigenvalues. Meanwhile, entries that do not contribute to signal generation are erased to enhance calculation efficiency. We decode the received signal using the pseudoinverse matrix and the removed pseudoinverse matrix to obtain the bit error rate performance and to analyze the difference.

**KEYWORDS**

binomial, cyclic, decoder, decomposition, division, frequency, multiplexing, OFDM, orthogonal, precoder, singular, spectrum

## 1 | INTRODUCTION

Orthogonal frequency division multiplexing (OFDM) has been used for decades in various fields, such as mobile communication [1], wireless local area network (WLAN) [2], satellite communication [3], broadcasting [4], and Internet of Things [5]. The reason is that OFDM is easy to implement through fast Fourier transform (FFT) and inverse fast Fourier transform (IFFT) and can effectively estimate and recover multipath fading channels. However, because OFDM has a square-shaped envelop [6], the power spectrum is spread, and the out-of-band emission (OoBE) power is leaked to the adjacent channel [7].

To suppress the spectral side lobe, the windowing for smoothing the transition of the OFDM envelope has been examined [8], but it does not sufficiently suppress the OoBE. Thus, technologies that can maintain the orthogonality between subcarriers to increase the bit error rate (BER) performance while suppressing the OoBE and inserting pilots have been developed [9–11]. These methods are relatively well handled mathematically but have high implementation complexity. A solution was proposed by considering OoBE suppression as a problem of minimizing the Frobenius norm of the matrix [12]. Although the weight vector is updated by reducing the OoBE through differentiation [13] to remove the discontinuity between successive OFDM symbols, continuous

errors may occur as it has a recursive structure. To reduce the OoBE and the peak-to-average power ratio of OFDM-based systems simultaneously, a method called alignment suppression was proposed [14]. This method requires a safe uplink channel because the transmitter uses channel state information and has a disadvantage because the implementation complexity for extracting the channel state information from the received signal is large. Methods [15–19] that can reduce the OoBE using the filter bank method have been proposed. However, these methods have various inherent problems, such as self-interference and difficulty in inserting pilot symbols. Consequently, filtered OFDM schemes that limit the OoBE by directly filtering OFDM symbols have been proposed [20, 21]. However, as the length of the filter is, at most, half of the length of the OFDM symbol, synchronization and BER performances may be negatively affected. Further, a method of reducing the OoBE using cancellation carriers has been proposed, and the receiver can demodulate the OoBE in the same manner as the conventional OFDM demodulation method [22]. Although this scheme maintains the transmission efficiency of existing OFDM, the spectrum characteristics are greatly improved when compared with the conventional scheme [23, 24] without self-interference. However, it must prove stability against insertion of cancellation carriers that are not used in existing standard technologies.

A technology that can completely prevent out-of-band power emission, which is the core technology of future wireless communication technology, has been proposed recently [25, 26]. These technologies developed spectrum encapsulation (SE)-OFDM based on three major technologies, namely, windowing, zero insertion, and orthogonalization, and implementation complexity was drastically reduced through vectorization [27]. Despite the maturity of the technology for blocking the OoBE of OFDM, whether it will continue to be used as a technology in the future remains questionable. This is mainly because communication channels in the future will become more complex than those in the present. For example, many buildings are built in narrow areas due to urbanization, and the multipath fading phenomenon increases because of an increase in transmission speed. In the currently used OFDM scheme, a cyclic prefix (CP) is used to overcome multipath fading. Despite the increase in future transmission speed, the CP length to overcome the multipath fading channel cannot be reduced because the transmission speed of radio waves remains unchanged. Therefore, for transmission efficiency, the ratio of the CP and data symbols is highly likely the same as that of the current method.

The binomial frequency division multiplexing (BFDM) scheme, which is a method of transmitting only the power required for data symbols, has been proposed for efficient information transmission [28]. It is designed to reduce the spread of the spectrum by allowing the columns of the system matrix to be composed of the coefficients of the binomial polynomial. When data symbols are transmitted in the time domain, BFDM symbols always start and end with zero. Additionally, the BFDM scheme has strong characteristics against collision and multipath fading channels when random access is performed. However, each column of the BFDM system matrix partially overlaps the neighboring column. In this case, interferences may occur between data symbols when data symbols are transmitted through a system matrix. The BER performance is expected to improve using complex algorithms. However, in-depth investigation is required to determine whether the performance sufficiently improves.

The properties of the BFDM system can be verified by finding the eigenvalues of the system matrix. That is, the eigenvalues of the matrix of the BFDM system are close to 1, resulting in an orthogonal matrix. Therefore, a little difference emerges in the ideal performance when using the least squares (LS) method than when using any other methods, and high-speed implementation is possible. However, a pseudoinverse matrix is required when performing the LS algorithm. According to the trend of technological development, the size of the transmission symbol tends to gradually increase [2]. Thus, the size of a system matrix inevitably increases, and the complexity of a transmitter and a receiver inevitably increases. This study aims to reduce the amount of computation by analyzing the properties of the pseudoinverse so that it can be applied to a large-scale BFDM system that operates at a high-speed in the future.

The following are the novelties and contributions of this paper:

① The system matrix is expressed as a linear sum of basis matrixes through single value decomposition (SVD).
② The existence of orthogonality between base matrixes is confirmed.
③ If the system matrix is a band matrix, then the basis matrix is a band matrix.
④ The pseudoinverse matrix can be expressed as the basis matrix of the system row and is proven as a band matrix. The erased pseudoinverse matrix is obtained by determining whether each entry contributes to the pseudoinverse matrix by setting an appropriate threshold value.
⑤ Using the eigenvalue of the system matrix, we evaluate the SIR performance when receiving the LS method at the receiver.

⑥ Decoding is possible by reducing the amount of calculation that confirms coincidence by calculating the BER performance obtained by the pseudoinverse and erased pseudoinverse matrixes.

As BFDM is a general form of OFDM, it can be applied to transmission methods based on OFDM (e.g., WLAN, DVBT, satellite, and LTE). BFDM can be applied for very complex cities or rugged mountainous terrains, and as it does not use CP, interference to neighboring channels can be reduced by communicating with low power. Further, because both matrixes $\mathbf{A}$ and $\mathbf{A}^+$ are band matrixes, implementation is quite easy.

The remainder of this paper is organized as follows. Section 2 introduces a communication system model that uses the BFDM method. Section 3 analyzes the properties of the BFDM system matrix through the SVD of the system matrix. Section 4 analyzes the properties of the pseudoinverse matrix and confirms that the matrix is a band matrix. Section 5 proposes a method to reduce the amount of decoding operations by deleting entries that have weak contributions to the operation using the BFDM system matrix as an example. In Section 6, the BER performance was evaluated when pseudoinverse and erased pseudoinverse matrixes were applied. Finally, Section 7 summarizes the results of the proposed method and suggests ways to apply it to various communication applications in the future.

## 2 | COMMUNICATION MODEL

Figure 1 presents the communication system model that applies the proposed scheme. A data vector is a vector comprising quadrature amplitude modulation symbols for each entry. It is multiplied by precoding matrix $\mathbf{A}$, and then IFFT is obtained and transformed from the frequency domain to the time domain and transmitted as a BFDM symbol. The channels are modeled using additive white Gaussian noise (AWGN) and multipath fading channels. The received symbol is transformed from the time to the frequency domain through FFT and then multiplied by decoding matrix $\mathbf{A}^+$ to restore the encoding function performed by the transmitter to the original matrix. The reconstructed symbol vector $w$ may be determined as a symbol vector close to the data vector after removing the distortion received from the channel to obtain an estimated data symbol.

If encoding matrix $\mathbf{A}$ and decoding matrix $\mathbf{A}^+$ are removed from the model in Figure 1, the proposed system reverts to the OFDM system. Therefore, this model can be considered a general communication model as an extended form of an OFDM system. The BFDM transmission symbol at time $k$ can be expressed as follows:

$$\mathbf{s}_k = \mathbf{F}_N^{\mathrm{H}} \mathbf{A} \mathbf{d}_k, \tag{1}$$

where $\mathbf{F}_N^{\mathrm{H}}$ is the inverse discrete Fourier transform matrix. The received signal is expressed as follows:

$$\mathbf{r}_k = \mathbf{C}_k \mathbf{s}_k + \mathbf{n}_k, \tag{2}$$

where $\mathbf{C}_k$ is the channel matrix and $\mathbf{n}_k$ is the AWGN noise vector.

As each column partially overlaps with neighboring columns in the BFDM system matrix, decoding using the LS method is preferred. Thus, the signal obtained can be expressed as

$$\begin{aligned} \mathbf{w}_k &= \mathbf{A}^+ \mathbf{F}_N \mathbf{r}_k \\ &= \mathbf{C}_k \mathbf{d}_k + \mathbf{A}^+ \tilde{\mathbf{n}}_k, \end{aligned} \tag{3}$$

where $\mathbf{A}^+$ is the pseudoinverse matrix and $\tilde{\mathbf{n}}_k = \mathbf{F}_N \mathbf{n}_k$ is the noise vector in the frequency domain.

In this study, we are not interested in channel $\mathbf{C}_k$, but we analyze the properties of pseudoinverse matrix $\mathbf{A}^+$ to reduce the implementation complexity of the receiver.

When the channel is ideal, the relation

$$\mathbf{A}^+ \mathbf{A} = \mathbf{I} \tag{4}$$

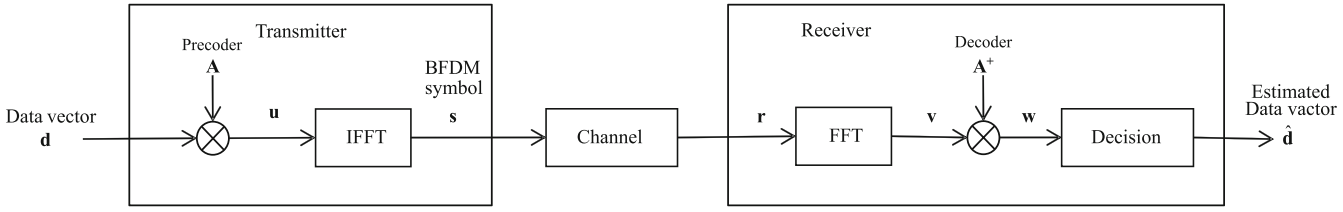


FIGURE 1 BFDM communication system model

should be satisfied.

## 3 | SYSTEM MATRIX

In the frequency domain, the BFDM system matrix can be expressed as a band matrix, as expressed in Equations (5) and (6). No upper bandwidth exists, and the lower bandwidth comprises two diagonal matrixes. Because many entries are zero, it can be observed that they have an efficient structure in terms of storage and calculation.

$$\mathbf{A} = \begin{bmatrix} \mathbf{0}_\alpha & \\ \mathbf{B}_+ & \mathbf{0}_\gamma \\ \mathbf{0}_\beta & \\ \mathbf{0}_\gamma & \mathbf{B}_- \end{bmatrix}, \tag{5}$$

where $\mathbf{0}_\alpha = \mathbf{0}^{(1\times M)}$, $\mathbf{0}_\beta = \mathbf{0}^{((N-2*(2M+1)-1)\times M)}$, and $\mathbf{0}_\gamma = \mathbf{0}^{((M+1)\times(M/2))}$. Here, $N$ is the number of subcarriers used, and $M$ is the length of the data vector to be transmitted. In general, data are transmitted using the number of subcarriers with an $M < N$ relationship and a larger number of transmitted data. The reason is that data utilize a subcarrier with a low-frequency subcarrier and tend not to use a high-frequency subcarrier. Here, $\mathbf{0}_\alpha$ and $\mathbf{0}_\beta$ indicate that DC subcarriers are not used and high-frequency subcarriers are not used, respectively, and $\mathbf{0}_\gamma$ serves to make space so that matrixes $\mathbf{B}_+$ and $\mathbf{B}_-$ can be positioned. System matrix $\mathbf{A}$ is a special matrix filled with a zero matrix between $\mathbf{B}_+$ and $\mathbf{B}_-$ comprising block matrix $\mathbf{B}$. The subcarriers of $\mathbf{B}_+$ and $\mathbf{B}_-$ comprise positive and negative subcarriers. However, their matrixes are identical, as expressed in (6). That is, (5) is a practically constructed form with matrix $\mathbf{B}$. In this paper, for brevity, only an example of using a second-order binomial polynomial [29] is given, but this can be explained with the same logic for third or more orders. For example, the positive and negative matrixes are defined as

$$\mathbf{B}_\pm = \frac{1}{\sqrt{6}} \begin{bmatrix} 1 & & & \\ 2 & 1 & & \\ 1 & 2 & & \\ & 1 & \ddots & \\ & & & 1 \\ & & & 2 \\ & & & 1 \end{bmatrix}, \tag{6}$$

$$\mathbf{A}^{(12\times 8)} = \frac{1}{\sqrt{6}} \begin{bmatrix} \mathbf{0} & & & & & & & \\ & 1 & & & & & & \\ & 2 & 1 & & & & & \\ & 1 & 2 & 1 & & & & \\ & & 1 & 2 & & & & \\ & & & 1 & & & & \\ & & & & \mathbf{0} & & & \\ & & & & & 1 & & \\ & & & & & 2 & 1 & \\ & & & & & 1 & 2 & 1 \\ & & & & & & 1 & 2 \\ & & & & & & & 1 \end{bmatrix}. \tag{7}$$

If matrix $\mathbf{B}$ can be modified in a dense mode, as expressed in (6), then matrix $\mathbf{A}$ can be represented in (7). Therefore, data length ($L_d$) and carrier length ($L_c$) are similar, resulting in CP-OFDM and similar transmission performance.

If matrix $\mathbf{B}$ is configured, as expressed in (6), then matrix $\mathbf{A}$ has a form of A (7). Therefore, the data and carrier lengths are similar, resulting in CP-OFDM and stunning performance. The relation between $L_d$ and $L_c$ is

$$L_c = L_d + 2. \tag{8}$$

If $L_d$ is sufficiently large, then this becomes $L_c \approx L_d$. That is, band-limited matrix $\mathbf{A}$ is able to suppress the interference from neighboring channels at the expense of very few carrier bands. That is, band-limiting matrix $\mathbf{A}$ is able to suppress the interference from neighboring channels at the expense of very few carrier bands.

The current CP-OFDM compensates for the channel through CP. Thus far, it has been used in almost all fields, such as LTE and WLAN. It is determined that multipath channels are overcome by allocating a CP length equal to 1/4 of the FFT size.

However, this method has two problems. First, the OFDM scheme is made in the scheme that is suitable for the AWGN environment. Therefore, as the multipath becomes longer, the length of the CP must be increased by the same amount. In CP-OFDM, if the multipath length is 1/2 of the total length due to the failure of urban buildings as cities develop, the CP length should be increased by 1/2 of the FFT size. Thus, transmission efficiency is reduced, and the power for the CP reaches half of the power for data transmission. Consequently, 1.5 times the power for the entire data transmission is required. Second, as CP-OFDM has a square wave envelope, it causes spectrum spread and presents interference

to neighboring cells. Although not adopted in 5G networks, many new waveforms, such as FBMC, F-OFDM, and GFDM, have been announced. Such methods based on filtering require more than twice the sampling rate of conventional methods because at least twice as many samples are required for filtering. In 6G networks, the current CP-OFDM method is not suitable because the transmission rate is very high and severe interference may be induced.

In the future, newly developed waveforms can be practically used only when high-speed transmission, interchannel interference, and low complexity are possessed. The BFDM scheme has such a characteristic. In this study, BFDM can be decoded using a simple LS method in such a context, which shows excellent performance.

For each column vector, $\mathbf{B} \in \mathbb{R}^{((2M+1)\times(M/2))}$ is obtained from the binomial polynomial. The SVDs of $\mathbf{A}$ and $\mathbf{B}$ may be expressed as

$$\mathbf{A} = \mathbf{U}_{\mathrm{A}} \mathbf{\Sigma}_{\mathrm{A}} \mathbf{V}_{\mathrm{T}}^{\mathrm{A}}, \tag{9a}$$

$$\mathbf{B} = \mathbf{U}_{\mathrm{B}} \mathbf{\Sigma}_{\mathrm{B}} \mathbf{V}_{\mathrm{T}}^{\mathrm{B}}, \tag{9b}$$

where $\mathbf{U}_{\mathrm{A}}$, $\mathbf{U}_{\mathrm{B}}$, $\mathbf{V}_{\mathrm{A}}$, and $\mathbf{V}_{\mathrm{B}}$ are unitary matrixes. Further, $\mathbf{\Sigma}_{\mathrm{A}}$ and $\mathbf{\Sigma}_{\mathrm{B}}$ are nonnegative diagonal matrixes as

$$\mathbf{\Sigma}_{\mathrm{A}} = \begin{bmatrix} \mathbf{Q}_{\mathrm{A}} \\ \mathbf{0} \end{bmatrix}, \tag{10a}$$

$$\mathbf{Q}_{\mathrm{A}} = \mathrm{diag}(\sigma_{\mathrm{A},1}, \ \sigma_{\mathrm{A},2}, \ L, \ \sigma_{\mathrm{A},M}), \tag{10b}$$

$$\mathbf{\Sigma}_{\mathrm{B}} = \begin{bmatrix} \mathbf{Q}_{\mathrm{B}} \\ \mathbf{0} \end{bmatrix}, \tag{11a}$$

$$\mathbf{Q}_{\mathrm{B}} = \mathrm{diag}\left(\sigma_{\mathrm{B},1}, \ \sigma_{\mathrm{B},2}, \ L, \ \sigma_{\mathrm{B},M/2}\right), \tag{11b}$$

and $\mathbf{0} \in \mathbb{R}^{((N-M)\times M)}$.

If $\mathbf{A}$ is expressed using eigenvectors, then it can be expressed as

$$\mathbf{A} = \sum_{s=1}^{M} \sigma_i \mathbf{u}_{\mathrm{A},i} \mathbf{v}_{\mathrm{A},i}^{\mathrm{T}}, \tag{12}$$

where $\mathbf{u}_{\mathrm{A},i}$ is the $i$th column vector of $\mathbf{U}$, $\mathbf{v}_{\mathrm{A},i}$ is the $i$th column vector of $\mathbf{V}$, and $\sigma_i$ is the $i$th eigenvalue of $\boldsymbol{A}$.

**Theorem 1.** *If matrix $\boldsymbol{A}$ is a band matrix, then matrixes*

$$\mathbf{\Phi}_i = \mathbf{u}_{\mathrm{A},i} \mathbf{v}_{\mathrm{A},i}^{\mathrm{T}} \quad i = 1, \ 2, \ L, \ M, \tag{13}$$

*are all band matrixes.*

*Proof.* If any of $\left\{\mathbf{u}_{\mathrm{A},i}\mathbf{v}_{\mathrm{A},i}^{\mathrm{T}} \mid i = 1, \ 2, \ L, \ M\right\}$ is not a band matrix, then $\mathbf{A}$, comprising a linear combination of positive coefficients $\{\sigma_{\mathrm{A},i} \mid i = 1, \ 2, \ L, \ M\}$, as expressed in (13) does not become a band matrix. Therefore, $\left\{\mathbf{u}_{\mathrm{A},i}\mathbf{v}_{\mathrm{A},i}^{\mathrm{T}} \mid i = 1, \ 2, \ L, \ M\right\}$ must all be band matrixes. □

**Theorem 2.** *Matrixes $\boldsymbol{\Phi}_i$ and $\boldsymbol{\Phi}_j$ are mutually orthogonal and are the basis matrixes constituting* $\mathbf{A}$.

*Proof.* Projecting $\boldsymbol{\Phi}_j$ to $\boldsymbol{\Phi}_i$, from Appendix A, we obtain

$$\mathbf{\Phi}_j^{\mathrm{T}} \mathbf{\Phi}_i = \begin{cases} \mathbf{I} & i = j \\ \mathbf{0} & i \neq j. \end{cases} \tag{14}$$

Here, $\{\mathbf{\Phi}_i \mid i = 1, \ 2, \ L, \ M\}$ are the basis matrixes for forming $\mathbf{A}$ because it is mutually orthogonal between matrixes. □

We can rewrite (12) as

$$\mathbf{A} = \sum_{s=1}^{M} \sigma_i \ \mathbf{\Phi}_i. \tag{15}$$

**Corollary 1.** *If matrix $\boldsymbol{A}$ is a band matrix, then its transpose matrix*

$$\begin{aligned} \mathbf{A}^{\mathrm{T}} &= \left( \sum_{s=1}^{M} \sigma_i \mathbf{\Phi}_i \right)^{\mathrm{T}} \\ &= \sum_{s=1}^{M} \sigma_i \mathbf{\Phi}_i^{\mathrm{T}} \end{aligned} \tag{16}$$

*is the band matrix. That is, $\mathbf{\Phi}_i^{\mathrm{T}}$ $(i = 1, \ 2, \ \Lambda, \ M)$ is a band matrix.*

*Proof.* According to **Theorem** 1, transpose matrix $\mathbf{A}^{\mathrm{T}}$ of $\mathbf{A}$ is in the form wherein the upper bandwidth is located at the position of the lower bandwidth and the lower bandwidth is located at the position of the upper bandwidth centering on the diagonal matrix. Therefore, the transpose matrix is a band

matrix because the band of the original matrix does not change. That is, if the original matrix is a band matrix, then the transpose matrix is also a band matrix. □

# 4 | PSEUDOINVERSE MATRIX OF THE SYSTEM MATRIX

## 4.1 | Pseudoinverse matrix

In this section, we analyze the pseudoinverse matrix of the system matrix for decoding A at the receive side. We consider the properties of the transpose matrix of system matrix **A**.

The left pseudoinverse matrix of **A** can be expressed as follows [30]:

$$\mathbf{A}^{+} = \left(\mathbf{A}^{\mathrm{T}}\mathbf{A}\right)^{-1}\mathbf{A}^{\mathrm{T}}. \tag{17}$$

**Theorem 3.** *If a matrix is a band matrix, then the pseudoinverse matrix is also a band matrix.*

*Proof.* From Appendix B, we obtain

$$\mathbf{A}^{+\mathrm{T}} = \frac{1}{M}\sum\nolimits_{r=1}^{M}\sigma_r\mathbf{\Phi}_r. \tag{18}$$

This matrix is a band matrix because it is a linear combination of matrixes, such as 10. According to Corollary 1, it is also a band matrix. □

From Appendix C, pseudoinverse matrix $\mathbf{A}^{+}$ can be expressed with $\mathbf{B}^{+}$ as

$$\mathbf{A}^{+} = \begin{bmatrix} \mathbf{0} & \mathbf{B}^{+} & \mathbf{0} & \mathbf{0} \\ \mathbf{0} & \mathbf{0} & \mathbf{0} & \mathbf{B}^{+} \end{bmatrix}, \tag{19}$$

where

$$\begin{aligned} \mathbf{B}^{+} &= \left(\mathbf{B}^{\mathrm{T}}\mathbf{B}\right)^{-1}\mathbf{B}^{\mathrm{T}} \\ &= \mathbf{V}_{\mathrm{B}}\mathbf{\Sigma}_{\mathrm{B}}^{+}\mathbf{U}_{\mathrm{B}}^{\mathrm{T}} \\ &= \sum_{i=1}^{M/2}\sigma_{\mathrm{B},i}\mathbf{v}_i\mathbf{u}_i. \end{aligned} \tag{20}$$

## 4.2 | Signal-to-interference ratio (SIR)

The Frobenius norm of **A** is

$$\begin{aligned} P_s = \|\mathbf{A}\|_{\mathrm{F}}^2 &= \left\| \begin{bmatrix} \mathbf{0} & \mathbf{0} \\ \mathbf{B} & \mathbf{0} \\ \mathbf{0} & \mathbf{0} \\ \mathbf{0} & \mathbf{B} \end{bmatrix} \right\|_{\mathrm{F}}^2 \\ &= 2\|\ \mathbf{B}\ \|_{\mathrm{F}}^2 \\ &= 2\left\|\mathbf{U}_{\mathrm{B}}\mathbf{\Sigma}_{\mathrm{B}}\mathbf{V}_{\mathrm{B}}^{\mathrm{T}}\right\|_{\mathrm{F}} \\ &= 2\|\mathbf{\Sigma}_{\mathrm{B}}\|_{F} \\ &= 2\times\frac{M}{2} \\ &= M. \end{aligned} \tag{21}$$

From Equations (17) and (18), the amount of power increase due to the pseudoinverse matrix of **A** is

$$\begin{aligned} P_{\mathrm{s}}^{+} &= \|\mathbf{A}^{+}\|_{\mathrm{F}}^2 \\ &= \left\| \begin{bmatrix} \mathbf{0} & \mathbf{B}^{+} & \mathbf{0} & \mathbf{0} \\ \mathbf{0} & \mathbf{0} & \mathbf{0} & \mathbf{B}^{+} \end{bmatrix} \right\|_{\mathrm{F}}^2 \\ &= 2\|\mathbf{B}^{+}\|_{\mathrm{F}}^2 \\ &= 2\sum_{i=1}^{M/2}\sigma_{\mathrm{B},i}^{-2}. \end{aligned} \tag{22}$$

Therefore, the SIR reduction due to the self-interference of the system matrix becomes

$$\gamma_{\mathrm{d}} = \frac{P_{\mathrm{s}}}{P_{\mathrm{s}}^{+}} = \frac{M}{2\sum_{i=1}^{M/2}\sigma_{\mathrm{B},i}^{-2}}. \tag{23}$$

## 4.3 | Eigenvalues of two diagonal matrixes

From Appendix D, the relation between two diagonal matrixes with eigenvalues $\mathbf{Q}_{\mathrm{A}}$ and $\mathbf{Q}_{\mathrm{B}}$ is

$$\mathbf{Q}_{\mathrm{A}} = \begin{bmatrix} \mathbf{Q}_{\mathrm{B}} & \\ & \mathbf{Q}_{\mathrm{B}} \end{bmatrix}. \tag{24}$$

To obtain the value of $\gamma_{\mathrm{d}}$, we should know the eigenvalues of matrix **B**. Obtaining the eigenvalues of **B** directly is difficult. Therefore, we want to find them in an indirect way. We have the product of $\mathbf{A}^{\mathrm{T}}$ and **A** as

$$\begin{aligned}\mathbf{\Lambda} &= \mathbf{A}^{\mathrm{T}}\mathbf{A} \\ &= \mathbf{V}_{\mathrm{A}}^{\mathrm{T}}\sum\nolimits_{\mathrm{A}}^{\mathrm{T}}\mathbf{U}_{\mathrm{A}}^{\mathrm{T}}\mathbf{U}_{\mathrm{A}}\sum\nolimits_{\mathrm{A}}\mathbf{V}_{\mathrm{A}} \\ &= \mathbf{V}_{\mathrm{A}}^{\mathrm{T}}\sum\nolimits_{\mathrm{A}}^{\mathrm{T}}\sum\nolimits_{\mathrm{A}}\mathbf{V}_{\mathrm{A}} \\ &= \mathbf{V}_{\mathrm{A}}^{\mathrm{T}}\sum\nolimits_{\mathrm{A}}^{2}\mathbf{V}_{\mathrm{A}}\end{aligned} \tag{25}$$

Meanwhile, (25) can be expressed as

$$\begin{aligned}\mathbf{\Lambda} &= \begin{bmatrix}\mathbf{0} & \mathbf{0}\\ \mathbf{B} & \mathbf{0}\\ \mathbf{0} & \mathbf{0}\\ \mathbf{0} & \mathbf{B}\end{bmatrix}^{\mathrm{T}}\begin{bmatrix}\mathbf{0} & \mathbf{0}\\ \mathbf{B} & \mathbf{0}\\ \mathbf{0} & \mathbf{0}\\ \mathbf{0} & \mathbf{B}\end{bmatrix} \\ &= \begin{bmatrix}\mathbf{0} & \mathbf{B}^{\mathrm{T}} & \mathbf{0} & \mathbf{0}\\ \mathbf{0} & \mathbf{0} & \mathbf{0} & \mathbf{B}^{\mathrm{T}}\end{bmatrix}\begin{bmatrix}\mathbf{0} & \mathbf{0}\\ \mathbf{B} & \mathbf{0}\\ \mathbf{0} & \mathbf{0}\\ \mathbf{0} & \mathbf{B}\end{bmatrix} \\ &= \begin{bmatrix}\mathbf{B}^{\mathrm{T}}\mathbf{B} & \mathbf{0}\\ \mathbf{0} & \mathbf{B}^{\mathrm{T}}\mathbf{B}\end{bmatrix}\end{aligned} \tag{26}$$

Evidently, the eigenvalues of matrix $\mathbf{\Lambda}$ are expressed as the square of the eigenvalues of matrix $\mathbf{B}$. Thus, after finding the eigenvalues, we can also find the eigenvalue of $\mathbf{B}$ by determining their square root.

Specifically, matrix $\mathbf{B}$ is can be expressed as

$$\mathbf{B} = \mathbf{U}_{\mathrm{B}}\mathbf{\Sigma}_{\mathrm{B}}\mathbf{V}_{\mathrm{T}}^{\mathrm{B}}. \tag{26}$$

By substituting (26) into (25), we obtain

$$\begin{aligned}\mathbf{\Lambda} &= \begin{bmatrix}\mathbf{V}_{\mathrm{B}}\mathbf{\Sigma}_{\mathrm{B}}\mathbf{U}_{\mathrm{B}}^{\mathrm{T}}\mathbf{U}_{\mathrm{B}}\mathbf{\Sigma}_{\mathrm{B}}\mathbf{V}_{\mathrm{B}}^{\mathrm{T}} & \\ & \mathbf{V}_{\mathrm{B}}\mathbf{\Sigma}_{\mathrm{B}}\mathbf{U}_{\mathrm{B}}^{\mathrm{T}}\mathbf{U}_{\mathrm{B}}\mathbf{\Sigma}_{\mathrm{B}}\mathbf{V}_{\mathrm{B}}^{\mathrm{T}}\end{bmatrix} \\ &= \begin{bmatrix}\mathbf{V}_{\mathrm{B}}\mathbf{\Sigma}_{\mathrm{B}}^{2}\mathbf{V}_{\mathrm{B}}^{\mathrm{T}} & \\ & \mathbf{V}_{\mathrm{B}}\mathbf{\Sigma}_{\mathrm{B}}^{2}\mathbf{V}_{\mathrm{B}}^{\mathrm{T}}\end{bmatrix} \\ &= \begin{bmatrix}\mathbf{V}_{\mathrm{B}} & \\ & \mathbf{V}_{\mathrm{B}}\end{bmatrix}\begin{bmatrix}\mathbf{\Sigma}_{\mathrm{B}}^{2} & \\ & \mathbf{\Sigma}_{\mathrm{B}}^{2}\end{bmatrix}\begin{bmatrix}\mathbf{V}_{\mathrm{B}}^{\mathrm{T}} & \\ & \mathbf{V}_{\mathrm{B}}^{\mathrm{T}}\end{bmatrix} \\ &= \begin{bmatrix}\mathbf{V}_{\mathrm{B}} & \\ & \mathbf{V}_{\mathrm{B}}\end{bmatrix}\left(\begin{bmatrix}\mathbf{\Sigma_{\mathrm{B}}} & \\ & \mathbf{\Sigma_{\mathrm{B}}}\end{bmatrix}\right)^{2}\begin{bmatrix}\mathbf{V}_{\mathrm{B}}^{\mathrm{T}} & \\ & \mathbf{V}_{\mathrm{B}}^{\mathrm{T}}\end{bmatrix}\end{aligned} \tag{27}$$

From (25) and (27), we obtain

$$\mathbf{\Sigma}_{2}^{\mathrm{A}} = \left(\begin{bmatrix}\mathbf{\Sigma}_{\mathrm{B}} & \\ & \mathbf{\Sigma}_{\mathrm{B}}\end{bmatrix}\right)^{2}. \tag{28}$$

Because the elements of $\mathbf{\Sigma}_{\mathrm{A}}$ are positive, we can take the positive solution

$$\mathbf{\Sigma}_{\mathrm{A}} = \begin{bmatrix}\mathbf{\Sigma}_{\mathrm{B}} & \\ & \mathbf{\Sigma}_{\mathrm{B}}\end{bmatrix}. \tag{29}$$

The following square matrix can be obtained using (6) directly as

$$\mathbf{\Lambda} = \frac{1}{6}\begin{bmatrix}6 & 4 & & & & & & & & & \\ 4 & 6 & 4 & & & & & & & & \\ & 4 & \ddots & 4 & & & & & & & \\ & & 4 & 6 & 4 & & & & & & \\ & & & 4 & 6 & & & & & & \\ & & & & & 6 & 4 & & & & \\ & & & & & 4 & 6 & 4 & & & \\ & & & & & & 4 & \ddots & 4 & & \\ & & & & & & & 4 & 6 & 4 & \\ & & & & & & & & 4 & 6 & \end{bmatrix}, \tag{30}$$

which is a typical tridiagonal matrix.

Applying the result of [25] to (30), the elements of $\mathbf{\Sigma}_{\mathrm{A}}$ given by (6) are

$$\begin{aligned}\Sigma_{\mathrm{B},i} &= \sqrt{\frac{1}{6}\left(6+2\cdot 4\cos\frac{\pi i}{M+1}\right)} \\ &= \sqrt{1+\frac{4}{3}\cos\frac{\pi i}{M+1}}, \\ \Sigma_{\mathrm{B},i+M/2} &= \Sigma_{\mathrm{B},i}, \quad i=1,\ 2,\ \Lambda,\ M/2.\end{aligned} \tag{31}$$

## 5 | ERASING THE ENTRIES

According to **Theorem** 1 and **Theorem** 2, $\mathbf{\Phi}_i$ is a band-based matrix, so $\mathbf{A}^{+\mathrm{T}}$ in Equation (13) is a band matrix. Accordingly, $\mathbf{A}^{+}$ is also a band matrix. In (13), when the eigenvalue is $\sigma_1 = \sigma_2 = \cdots = \sigma_M = 1$, the system matrix has an important meaning. The reason is that in the case of $i \neq j$, $\mathbf{\Phi}_i$ and $\mathbf{\Phi}_j$ are orthogonal, so all sums of the base matrixes can be a criterion for estimating the bandwidth.

From (13), we have

$$\mathbf{A}|_{\sigma_1=\sigma_2=\mathrm{L}\ =\sigma_M=1}=\sum_{s=1}^{M}\sigma_i\mathbf{\Phi}_i|_{\sigma_1=\sigma_2=\mathrm{L}\ =\sigma_M=1}=\sum_{i=1}^{M}\mathbf{\Phi}_i. \tag{32}$$

From (16), we obtain

$$\mathbf{A}_+\equiv\mathbf{A}^{+\mathrm{T}}|_{\sigma_1=\sigma_2=\mathrm{L}\ =\sigma_M=1}=\sum_{i=1}^{M}\sigma_i^{-1}\mathbf{\Phi}_i|_{\sigma_1=\sigma_2=\mathrm{L}\ =\sigma_M=1}=\sum_{i=1}^{M}\mathbf{\Phi}_i. \tag{33}$$

With

$$\mathbf{A}_\mathrm{o}=\frac{1}{\sqrt{M}}\mathbf{A}_+, \tag{34}$$

it can be observed from Appendix E that $\mathbf{A}_\mathrm{o}$ is an orthogonal matrix. Meanwhile, $\mathbf{A}^+$ has the same bandwidth as $\mathbf{A}$, and $\mathbf{A}^+$ is a band matrix. Figure 4 shows orthogonal matrixes $\mathbf{A}_\mathrm{o}$ and $\mathbf{A}^+$. As shown in the figure, although a slight difference exists, the arrangement of $\mathbf{A}_\mathrm{o}$ is more regular than that of $\mathbf{A}^+$. The reason is that the eigenvalues of $\mathbf{A}^+$ are irregular, whereas those of $\mathbf{A}_\mathrm{o}$ are constant at 1. Therefore, using $\mathbf{A}_\mathrm{o}$ may be more convenient than using $\mathbf{A}^+$ to estimate the bandwidth of the matrix. Meanwhile, the nearest orthogonal matrix $\mathbf{A}_\perp$ of $\mathbf{A}$ can be obtained directly by the following equation [27]:

$$\mathbf{A}_\perp=\mathbf{A}\left(\mathbf{A}^\mathrm{T}\mathbf{A}\right)^{-\frac{1}{2}}. \tag{35}$$

Latter matrix $\left(\mathbf{A}^\mathrm{T}\mathbf{A}\right)^{-1/2}$ serves to change the eigenvalues of previous matrix $\mathbf{A}$ to 1, and Equation (35) becomes

$$\mathbf{A}_\perp=\mathbf{U}_\mathrm{A}\begin{bmatrix}\mathbf{I}\\ \mathbf{0}\end{bmatrix}\mathbf{V}_\mathrm{A}^\mathrm{T}, \tag{36}$$

where the sizes of $\mathbf{I}$ and $\mathbf{0}$ are $M\times M$ and $(N-M)\times M$, respectively. Evidently, matrix $\mathbf{A}_\perp$ is an orthogonal matrix. The following relation is established as

$$\mathbf{A}_\mathrm{o}=\mathbf{A}_\perp^\mathrm{T}. \tag{37}$$

In Figure 2, the color change depending on the value of the $Z$-axis, which is the height, is inconvenient to view.

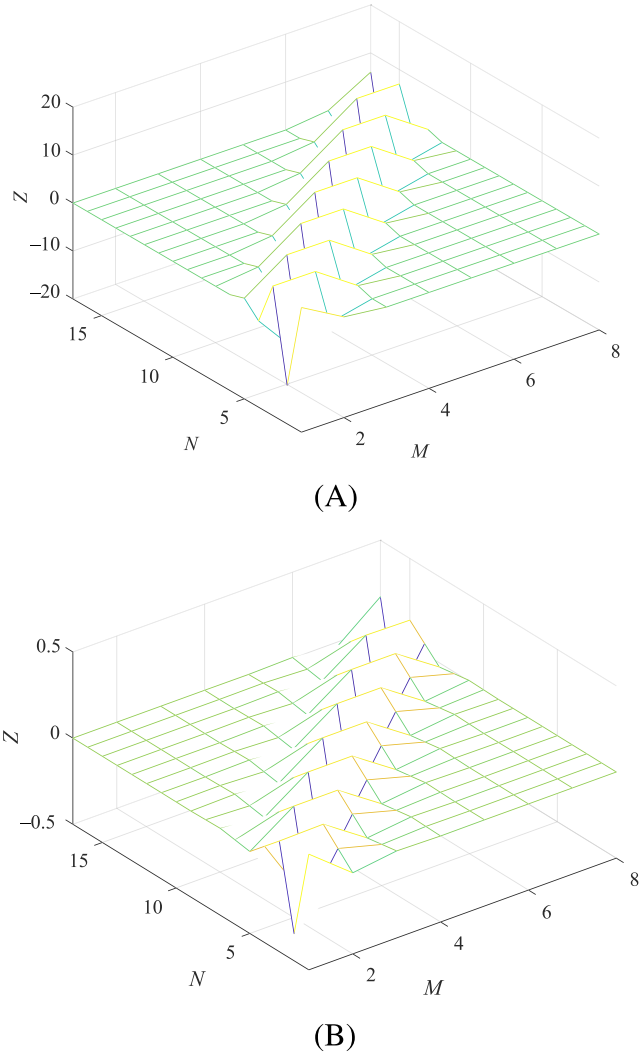


**FIGURE 2** System matrix-related matrixes. (A) Orthogonal matrix $\mathbf{A}_\mathrm{o}$ and (B) pseudoinverse matrix $\mathbf{A}^+$, where $N=17$, $M=8$

Hence, the angle was changed to adjust the cubic curve to be discernible. In the figure, eight data are transmitted using 17 subcarriers. Further, both matrixes are band matrixes because they have valid values on the diagonal.

**Theorem 4.** *The bandwidth of band matrix* $\boldsymbol{A}$ *and pseudoinverse matrix* $\boldsymbol{A}^+$ *is always constant regardless of the matrix size.*

*Proof.* If matrix $\mathbf{A}$ is a band matrix, the bandwidth is constant regardless of the size of the matrix. The orthogonal matrixes of $\mathbf{A}$ and $\mathbf{A}^{+\mathrm{T}}$ are the same as those from (13) and (16). Therefore, the bandwidth of $\mathbf{A}^+$ is the same as that of $\mathbf{A}^\mathrm{T}$. That is, regardless of the size of matrix $\mathbf{A}^+$, the bandwidth is constant. □

All entries are erased to zero, except for the number of entries in the bandwidth. By doing this, we want to exclude an entry with a value of 0 from the LS operation. The efficiency obtained by reducing the amount of calculation from **Theorem** 1 to **Theorem** 4 can be calculated as the ratio of the number of zeros and total number of entries as follows.

$$\eta = \frac{NM - \alpha M}{NM} = 1 - \frac{\alpha}{2M+1}, \tag{38}$$

where $\alpha$ is the diagonal bandwidth of the inverse matrix and the relation of $N = 2M + 1$ is utilized. Figure 3 shows the efficiency according to $M$. Clearly, the efficiency approaches 1 as $M$ increases. As the size of the pseudoinverse matrix increases, the number of entries with a value of 0 increases. Hence, efficiency can be improved by reducing the amount of computation.

The complexity of the system matrix is determined by matrixes $\mathbf{A}$ and $\mathbf{A}^+$. This study reveals that these matrixes are band matrixes. In the range that does not affect the BER performance as in the question, complexity improvement did not affect the BER performance near 80%. Therefore, when designing a system, we recommend a method that can find alpha, $M$, and $N$ by investigating in the vicinity (e.g., from 75% to 85% eta) that does not degrade the complexity and original BER performance. In this study, when eta is 79%, the BER performance is identical to that of the original $\mathbf{A}^+$ decoding method, indicating that it is an optimal method. However, the optimal general formula remains under investigation.

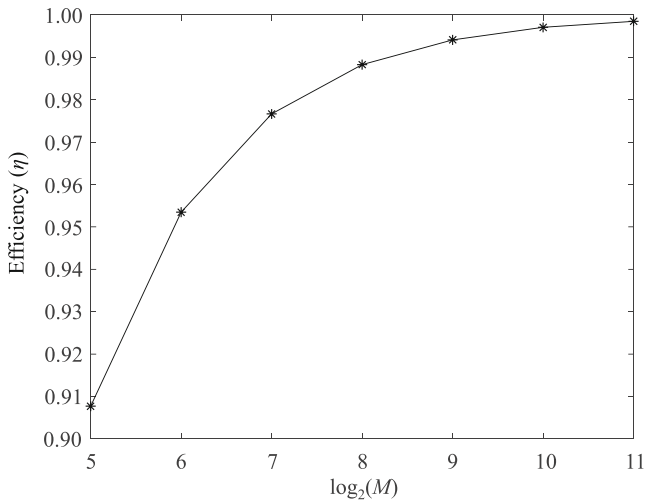


**FIGURE 3** Reduction efficiency ($\eta$) of pseudoinverse matrix $\mathbf{A}^+$ with $\alpha = 6$

## 6 | BER PERFORMANCE

It is crucial to show that although an erased pseudoinverse matrix is obtained through a mathematically

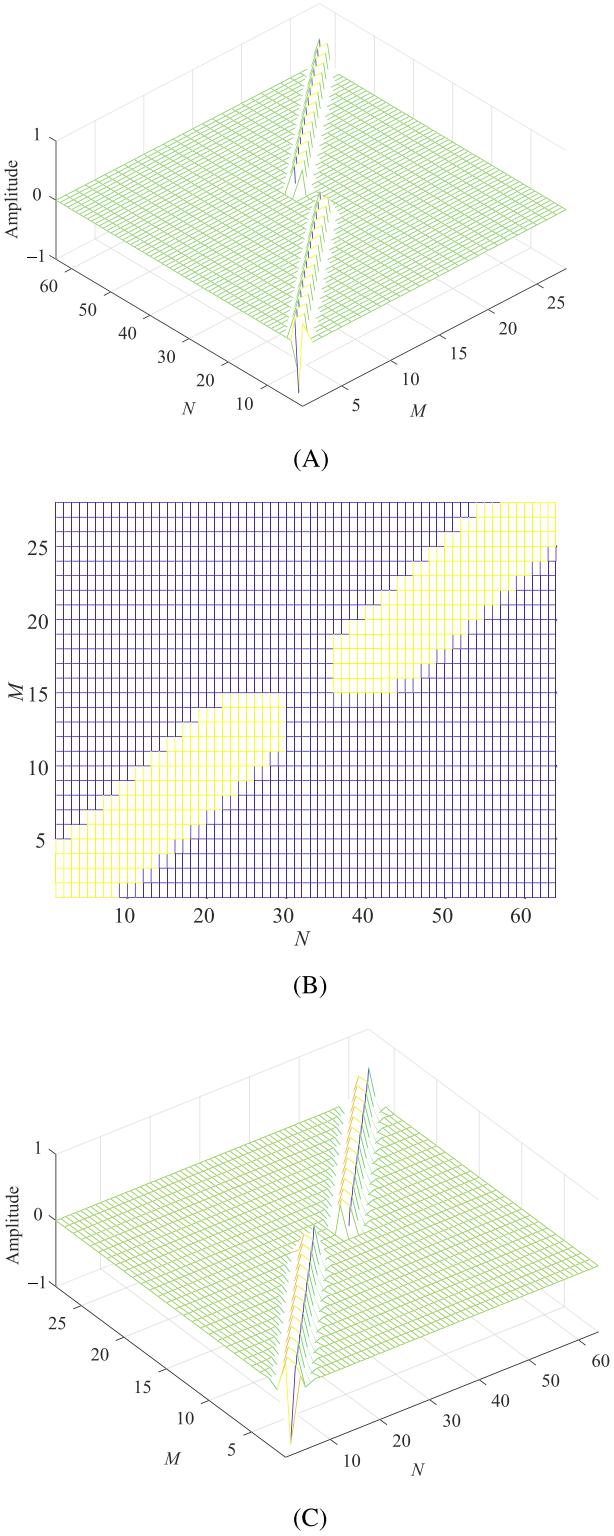


**FIGURE 4** System matrix-related matrixes with $M = 28$ and $N = 64$. (A) System matrix. (B) Selected area. (C) Erased pseudoinverse matrix

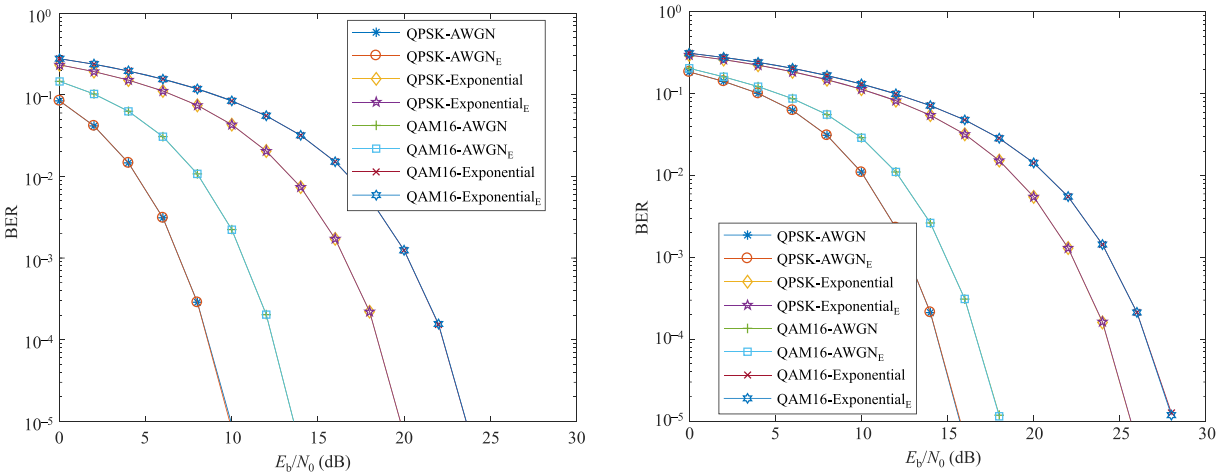


**FIGURE 5** BER performance. (A) QPSK and 16QAM and (B) 32QAM and 64QAM. Subscript E in the legend denotes the "erased" mode.

rigorous process, it is applied to an actual BFDM receiver to demonstrate that its functionality or performance does not weaken. Therefore, in this section, we attempt to analyze the performance with a relatively small system matrix that is easy to reproduce.

The parameters of the system matrix used for BER performance analysis are as follows:

$$\alpha = 12,$$

$$M = 28.$$

Here, $\alpha$ is the bandwidth of the bandwidth of the system matrix, and all entries outside the band are set to 0 and are excluded from the actual operation. According to Equation (32), when $\alpha$ is 0, the complexity improvement efficiency $\eta$ becomes 1. When $\alpha = 12$ and $M = 28$, $\eta$ is $1-12/(2\times 28+1) = 79$. The BER was measured in this environment.

Figure 4 shows the process of obtaining the erased matrix from the system matrix. Figure 4A–C show the system matrix, entry with the size of the orthogonal matrix larger than 0.0018, and erased pseudoinverse matrix, respectively. As shown in Figure 4B, there are far more entries that do not contribute than entries that contribute to decoding.

Figure 5 shows the BER performances when decoding is performed using the pseudoinverse and erased pseudoinverse matrixes. As shown in Figure 5B, as the number of 1 s is 368, the number of multiplications contributing to decoding is 368 at a matrix size of 28 × 64. However, the remaining 0 s do not contribute to decoding and can be omitted during implementation. Therefore, the implementation efficiency is $368/(28\times 64) = 0.7946$. The BER performances of the exact and reduced pseudoinverse mode are obtained and compared through the AWGN channel and the exponentially delayed multipath fading channel $h(k) = C\cdot 10^{-k/10}$, $k = 0,1,...,31$ [26], where $C$ is the power normalization factor.

The performances of the two modes obtained through the simulation are indistinguishably consistent. Therefore, it was confirmed that despite that the erased mode is applied, it can be implemented without performance deterioration.

This result indicates that if the system matrix is a band matrix, the pseudoinverse matrix is also a band matrix, and the complexity of implementation can be reduced by applying the erased method.

Refer to [28] for a comparison of the BER performances of OFDM and BFDM over AWGN and multipath fading channel.

This paper presents a scheme to reduce the complexity of the LS method. In addition to the efficiency for the complexity of the proposed method, the BER performance should be proven not to degrade the performance of existing methods. As shown in the BER performance presented in Figure 5, the performances of the original method and the proposed method are accurate that they cannot be distinguished with the naked eye.

## 7 | CONCLUSION

In this study, we analyzed the characteristics of the self-interference of the BFDM system and the pseudoinverse matrix required when applying the LS technique for

signal decoding in the receiving system. We confirmed that the BFDM system matrix and its pseudoinverse matrix are both band matrixes. In the process, the system matrix was decomposed by SVD to extract the left and right singular vectors. We confirmed that the matrixes comprising the product of such vectors are orthogonal to each other and are band matrixes. It was also proved that the bandwidth was independent of the system matrix size, and the computational efficiency according to the number of transmission symbols was obtained on this basis. In general, the LS method is used during demodulation, and if the system matrix is large, implementation complexity becomes quite high as well; thus, it is not suitable as a future transmission technology. BFDM can meet the high-speed transmission required by future technology and can overcome a multipath fading environment. Through this study, it not only maintains compatibility with existing transmission technologies but also establishes a theoretical foundation for the development of various new transmission technologies.

## CONFLICT OF INTEREST STATEMENT

The authors declare that there are no conflicts of interest.

## ORCID

*Myungsup Kim* https://orcid.org/0000-0003-3344-2545

## REFERENCES

1. LTE; Evolved universal terrestrial radio access (E-UTRA); user equipment (UE) radio transmission and reception (3GPP TS 36.101 version 10.3.0 release 10), ETSI TS 136 101 V10.3.0, 2011-06.
2. Specification framework for TGax, IEEE 802.11-15/0132r15.
3. A. Papathanassiou, A. K. Salkintzis, and P. T. Mathiopoulos, *A comparison study of the uplink performance of W-CDMA and OFDM for mobile multimedia communications via LEO satellites*, IEEE Pers. Commun. **8** (2001), no. 3, 35–43.
4. Digital Video Broadcasting (DVB). Transmission system for handheld terminals (DVB-H), ETSI (2004), EN 302304 v1.1.1.
5. L. Cho, X. H. Yu, C. Y. Chen, and C. Y. Hsu, *Green OFDM for IoT: Minimizing IBO subject to a spectral mask*, (IEEE International Conference on Applied System Invention, Chiba, Japan), 2018, pp. 13–17. https://doi.org/10.1109/ICASI.2018.8394252
6. D. Qu, J. Ding, T. Jiang, and X. Sun, *Detection of non-contiguous OFDM symbols for cognitive radio systems without out-of-band spectrum synchronization*, IEEE Trans. Wirel. Commun. **10** (2011), no. 2, 693–701.
7. A. Sahin, I. Güvenç, and H. Arslan, *A survey on multicarrier communications: Prototype filters, lattice structures, and implementation aspects*, IEEE Commun. Tut. **16** (2014), no. 3, 1312–1338.
8. A. Sahin and H. Arslan, *Edge windowing for OFDM based systems*, IEEE Commun. Lett. **15** (2011), no. 11, 1208–1211.
9. C.-D. Chung, *Spectral precoding for rectangular pulsed OFDM*, IEEE Trans. Commun. **59** (2008), no. 9, 1498–1510.
10. C.-D. Chung and K.-W. Chen, *Spectrally precoded OFDM without guard insertion*, IEEE Trans. Veh. Technol. **66** (2017), no. 1, 107–121.
11. W.-C. Chen and C.-D. Chung, *Spectrally efficient OFDM pilot waveform for channel estimation*, IEEE Trans. Commun. **65** (2017), no. 1, 387–402.
12. M. Ma, X. Huang, B. Jiao, and Y. J. Guo, *Optimal orthogonal precoding for power leakage suppression in DFT-based systems*, IEEE Trans. Commun. **59** (2011), no. 3, 387–402.
13. J. van de Beek and F. Berggren, *N-continuous OFDM*, IEEE Commun. Lett. **13** (2009), no. 1, 1–3.
14. A. Tom, A. Şahin, and H. Arslan, *Suppressing alignment: Joint PAPR and out-of-band power leakage reduction for OFDM-based systems*, IEEE Trans. Commun. **64**, no. 3, 1100–1109.
15. B. Farhang-Boroujeny, *OFDM versus filter bank multicarrier*, IEEE Signal Process. Mag. **28** (2011), no. 3, 92–112.
16. R. Datta, N. Michailow, M. Lentmaier, and G. Fettweis, *GFDM interference cancellation for flexible cognitive radio PHY design*, (IEEE Vehicular Technology Conference, Quebec, Canada), 2021, pp. 1–5.
17. J. K. Jeong, Y. S. Park, S. W. Weon, J. T. Kim, S. Y. Choi, and D. S. Hong, *Eigendecomposition-based GFDM for interference-free data transmission and pilot insertion for channel estimation*, IEEE Trans. Wireless Commun. **17** (2018), no. 10, 6931–6943.
18. F. Li, K. Zheng, L. Zhao, H. Zhao, and Y. Li, *Design and performance of a novel interference-free GFDM transceiver with dual filter*, IEEE Trans. VT. **68** (2019), no. 5, 3045–3061.
19. J. Abdoli, M. Jia, and J. Ma, *Filtered OFDM, a new waveform for future wireless systems*, (IEEE 16th International Workshop on Signal Processing Advanceds iin Wireless Communications, Stockhlom, Sweden), 2015. https://doi.org/10.1109/SPAWC.2015.7227001
20. H. Chen, J. Hua, F. Li, F. Chen, and D. Wang, *Interference analysis in the asynchronous f-OFDM systems*, IEEE Trans. Commun. **67** (2019), no. 5, 3580–3596.
21. L. Díez, J. A. Cortés, F. J. Cañete, E. Martos, and S. Iranzo, *A generalized spectral shaping method for OFDM signals*, IEEE Trans. Commun. **67** (2019), no. 5, 3540–3551.
22. J. A. C. Bingham, *RFI suppression in multicarrier transmission systems*, (Proceedings of the IEEE Global Telecommunications Conference, London, UK), 1996, pp. 1026–1030.
23. T. Weiss, J. Hillenbrand, A. Krohn, and F. K. Jondral, *Mutual interference in OFDM-based spectrum pooling systems*, (IEEE 59th Vehicular Technology Conference, Milan, Italy), 2004, pp. 1873–1877.
24. D. Qu, A. Wang, and T. Jiang, *Extended active interference cancellation for sidelobe suppression in cognitive radio OFDM systems with cyclic prefix*, IEEE Trans. Veh. Tech. **59** (2010), no. 4, 1689–1695.
25. M. S. Kim, D. Y. Kwak, J. W. Jung, and K. M. Kim, *Spectral encapsulation of OFDM: Vectorized structure with minimal complexity*, ETRI J. (2020), 660–673.
26. M. S. Kim, D. Y. Kwak, K. M. Kim, and W. J. Kim, *Spectral encapsulation of OFDM systems based on orthogonalization for short packet transmission*, ETRI J. **42** (2020), 859–871. https://doi.org/10.4218/etrij.2019-0307

27. M. S. Kim, J. W. Jung, D. Y. Kwak, K. M. Kim, and W. J. Kim, *Spectral encapsulation to block the out-of-band emission of OFDM signals for future communications*, (IEEE 91st Vehicular Technology Conference, Antwerp, Belguim), 2020. https://doi.org/10.1109/VTC2020-Spring48590.2020.9129421
28. M. S. Kim, D. Y. Kwak, and K. M. Kim, *Binomial frequency division multiplexing: noble waveform with spectral efficiency and robustness to multipath fading*, (VTC 2019-Spring), May. 2019.
29. M. S. Kim, J. S. Seong, M. A. Joong, and S. R. Lee, *Multinomial filter*, (International Conference on Information and Communication Technology Convergence, Busan Rep. of Korea), 2014. https://doi.org/10.1109/ICTC.2014.6983301
30. https://en.wikipedia.org/wiki/Moore%E2%80%93Penrose_inverse, WIKIPEDIA.

## AUTHOR BIOGRAPHIES

**Myungsup Kim** received his BS degree in electronic engineering from Han Yang University, Seoul, Republic of Korea, in 1986, his MS degree in electronic engineering from Chungnam National University, Republic of Korea, in 1991, and his PhD degree in information and communication engineering from Korea Advanced Institute of Science and Technology (KAIST), Seoul, Republic of Korea, in 1999. From 1986 to 2000, he worked for the Electronics and Telecommunications Research Institute, Daejeon, Republic of Korea. From 2001 to 2014, he worked for Tunitel Co., Daejeon, Republic of Korea. From 2015 to 2019, he worked for the Department of Mathematical Sciences, KAIST, Daejeon, Republic of Korea. Since 2020, he has been with Korea Maritime and Ocean University, Busan, Republic of Korea, where he is now a contract professor. His main research interests include communication theory and signal processing for future wireless and underwater acoustic communications.

**Jiwon Jung** received his BS, MS, and PhD degrees in electronic engineering from Sungkyunkwan University, Seoul, Republic of Korea, in 1989, 1991, and 1995, respectively. From November 1990 to February 1992, he was with the LG Research Center, Anyang, Republic of Korea. From September 1995 to August 1996, he was with Korea Telecom, Seoul, Republic of Korea. From August 2001 to July 2002, he was an Invited Researcher with the Communication Research Center Canada (supported by Natural Sciences and Engineering Research Council of Canada). Since 1996, he has been with the Department of Radio Communication Engineering, Korea Maritime and Ocean University, Busan, Republic of Korea, where he is now a professor. His main research interests include channel coding theory, digital broadcasting systems, and underwater acoustic communications.

**Ki-Man Kim** received his BS, MS, and PhD degrees in electronic engineering from Yonsei University, Seoul, Republic of Korea, in 1988, 1990, and 1995, respectively. He was a fellow at Yonsei Medical Center from 1995 to 1996. Since 1996, he has been with the Department of Radio Communication Engineering, Korea Maritime and Ocean University, Busan, Republic of Korea, where he is now a professor. His main research interests include array signal processing, underwater acoustic/laser communications, and sonar localization.

**How to cite this article:** M. Kim, J. Jung, and K.-M. Kim, *Least squares decoding in binomial frequency division multiplexing*, ETRI Journal **45** (2023), 277–290. https://doi.org/10.4218/etrij.2021-0456

## APPENDIX A: ORTHOGONALITY OF BASE MATRIXES

Projecting $\mathbf{\Phi}_j$ onto $\mathbf{\Phi}_i$, the resultant matrix becomes

$$\begin{aligned}\left(\mathbf{\Phi}_j\right)^{\mathrm{T}}\mathbf{\Phi}_i &= \mathbf{\Phi}_j^{\mathrm{T}}\mathbf{\Phi}_i \\ &= \left(\mathbf{u}_j\mathbf{v}_j^{\mathrm{T}}\right)^{\mathrm{T}}\mathbf{u}_i\mathbf{v}_i^{\mathrm{T}} \\ &= \mathbf{v}_j\mathbf{u}_j^{\mathrm{T}}\mathbf{u}_i\mathbf{v}_i^{\mathrm{T}}.\end{aligned} \tag{A1}$$

(i) In case $i = j$

Matrix $\mathbf{U}$ is a unitary matrix; hence, $\mathbf{u}_i^{\mathrm{T}}\mathbf{u}_i = \mathbf{I}^{(M\times M)}$. Substituting this into (A1) yields

$$\begin{aligned}\mathbf{\Phi}_i^{\mathrm{T}}\mathbf{\Phi}_i &= \mathbf{v}_i\mathbf{I}^{(M\times M)}\mathbf{v}_i^{\mathrm{T}} \\ &= \mathbf{v}_i\mathbf{v}_i^{\mathrm{T}} \\ &= \mathbf{I}^{(M\times M)}.\end{aligned} \tag{A2}$$

(ii) In case $i \neq j$

As matrix $\mathbf{U}$ is a unitary matrix, $\mathbf{u}_i$ and $\mathbf{u}_j$ are orthogonal to each other. Thus, (A1) becomes

$$\begin{aligned}\boldsymbol{\Phi}_j^{\mathrm{T}}\boldsymbol{\Phi}_i &= \mathbf{v}\mathbf{0}^{(M\times M)}\mathbf{v}_i^{\mathrm{T}}\\ &= \mathbf{0}^{(M\times M)}\mathbf{v}_i^{\mathrm{T}}\\ &= \mathbf{0}^{(M\times M)}.\end{aligned} \tag{A3}$$

From i) and ii), the results can be summarized as

$$\boldsymbol{\Phi}_j^{\mathrm{T}}\boldsymbol{\Phi}_i = \begin{cases}\mathbf{I} & i=j\\ \mathbf{0} & i\neq j.\end{cases} \tag{A4}$$

## APPENDIX B: TRANSPOSED PSEUDOINVERSE OF THE SYSTEM MATRIX

When (12) is substituted into (14), the pseudoinverse matrix can be written as

$$\begin{aligned}\mathbf{A}^{+} &= \left(\sum_{p=1}^{M}\sigma_p\boldsymbol{\Phi}_p\right)^{\mathrm{T}}\left(\sum_{q=1}^{M}\sigma_q\boldsymbol{\Phi}_q\right)\right)^{-1}\left(\sum_{r=1}^{M}\sigma_r\boldsymbol{\Phi}_r\right)^{\mathrm{T}}\\ &= \left(\left(\sum_{p=1}^{M}\sigma_p\boldsymbol{\Phi}_p^{\mathrm{T}}\right)\left(\sum_{p=1}^{M}\sigma_q\boldsymbol{\Phi}_q\right)\right)^{-1}\left(\sum_{p=1}^{M}\sigma_r\boldsymbol{\Phi}_r^{\mathrm{T}}\right)\\ &= \left(\sum_{p=1}^{M}\sum_{q=1}^{M}\sigma_p\sigma_q\boldsymbol{\Phi}_p^{\mathrm{T}}\boldsymbol{\Phi}_q\right)^{-1}\left(\sum_{p=1}^{M}\sigma_r\boldsymbol{\Phi}_r^{\mathrm{T}}\right).\end{aligned} \tag{B1}$$

By applying (11) to (B1), we obtain

$$\begin{aligned}\mathbf{A}^{+} &= \left(\sum_{p=1}^{M}\sigma_p^2\mathbf{I}\right)^{-1}\left(\sum_{r=1}^{M}\sigma_r\boldsymbol{\Phi}_r^{\mathrm{T}}\right)\\ &= \left(\sum_{p=1}^{M}\sigma_p^2\right)^{-1}\mathbf{I}\left(\sum_{r=1}^{M}\sigma_r\boldsymbol{\Phi}_r^{\mathrm{T}}\right)\\ &= M^{-1}\left(\sum_{r=1}^{M}\sigma_r\boldsymbol{\Phi}_r^{\mathrm{T}}\right)\\ &= \frac{1}{M}\sum_{r=1}^{M}\sigma_r\boldsymbol{\Phi}_r^{\mathrm{T}}.\end{aligned} \tag{B2}$$

Taking the transpose on both sides of (B2), the transpose of $\mathbf{A}^{+}$ becomes

$$\mathbf{A}^{+\mathrm{T}} = \frac{1}{M}\sum_{r=1}^{M}\sigma_r\boldsymbol{\Phi}_r. \tag{B3}$$

## APPENDIX C: PSEUDOINVERSE OF THE SYSTEM MATRIX

By substituting (5) into (4), with (12), we get

$$\begin{aligned}\mathbf{A}^{+} &= \left(\begin{bmatrix}\mathbf{0} & \mathbf{B}^{\mathrm{T}} & \mathbf{0} & \mathbf{0}\\ \mathbf{0} & \mathbf{0} & \mathbf{0} & \mathbf{B}^{\mathrm{T}}\end{bmatrix}\begin{bmatrix}\mathbf{0} & \mathbf{0}\\ \mathbf{B} & \mathbf{0}\\ \mathbf{0} & \mathbf{0}\\ \mathbf{0} & \mathbf{B}\end{bmatrix}\right)^{-1}\begin{bmatrix}\mathbf{0} & \mathbf{B}^{\mathrm{T}} & \mathbf{0} & \mathbf{0}\\ \mathbf{0} & \mathbf{0} & \mathbf{0} & \mathbf{B}^{\mathrm{T}}\end{bmatrix}\\ &= \begin{bmatrix}\mathbf{B}^{\mathrm{T}}\mathbf{B} & \mathbf{0}\\ \mathbf{0} & \mathbf{B}^{\mathrm{T}}\mathbf{B}\end{bmatrix}^{-1}\begin{bmatrix}\mathbf{0} & \mathbf{B}^{\mathrm{T}} & \mathbf{0} & \mathbf{0}\\ \mathbf{0} & \mathbf{0} & \mathbf{0} & \mathbf{B}^{\mathrm{T}}\end{bmatrix}\\ &= \begin{bmatrix}\left(\mathbf{B}^{\mathrm{T}}\mathbf{B}\right)^{-1} & \mathbf{0}\\ \mathbf{0} & \left(\mathbf{B}^{\mathrm{T}}\mathbf{B}\right)^{-1}\end{bmatrix}\begin{bmatrix}\mathbf{0} & \mathbf{B}^{\mathrm{T}} & \mathbf{0} & \mathbf{0}\\ \mathbf{0} & \mathbf{0} & \mathbf{0} & \mathbf{B}^{\mathrm{T}}\end{bmatrix}\\ &= \begin{bmatrix}\mathbf{0} & \left(\mathbf{B}^{\mathrm{T}}\mathbf{B}\right)^{-1}\mathbf{B}^{\mathrm{T}} & \mathbf{0} & \mathbf{0}\\ \mathbf{0} & \mathbf{0} & \mathbf{0} & \left(\mathbf{B}^{\mathrm{T}}\mathbf{B}\right)^{-1}\mathbf{B}^{\mathrm{T}}\end{bmatrix}\\ &= \begin{bmatrix}\mathbf{0} & \mathbf{B}^{+} & \mathbf{0} & \mathbf{0}\\ \mathbf{0} & \mathbf{0} & \mathbf{0} & \mathbf{B}^{+}\end{bmatrix},\end{aligned} \tag{C1}$$

where

$$\mathbf{B}^{+} = \left(\mathbf{B}^{\mathrm{T}}\mathbf{B}\right)^{-1}\mathbf{B}^{\mathrm{T}}. \tag{C2}$$

By substituting (6b) into (C2), we obtain

$$\mathbf{B}^{+} = \mathbf{V}_{\mathrm{B}}\boldsymbol{\Sigma}_{\mathrm{B}}^{+}\mathbf{U}_{\mathrm{B}}^{\mathrm{T}}. \tag{C3}$$

## APPENDIX D: EIGENVALUE MATRIX OF THE SYSTEM MATRIX

With (6a) and (7a), we obtain

$$\begin{aligned}\mathbf{A}^{\mathrm{T}}\mathbf{A} &= \left(\mathbf{U}_{\mathrm{A}}\boldsymbol{\Sigma}_{\mathrm{A}}\mathbf{V}_{\mathrm{A}}^{\mathrm{T}}\right)^{\mathrm{T}}\left(\mathbf{U}_{\mathrm{A}}\boldsymbol{\Sigma}_{\mathrm{A}}\mathbf{V}_{\mathrm{A}}^{\mathrm{T}}\right)\\ &= \mathbf{V}_{\mathrm{A}}\mathbf{Q}_{\mathrm{A}}^{2}\mathbf{V}_{\mathrm{A}}^{\mathrm{T}}.\end{aligned} \tag{D1}$$

With (4), we obtain

$$\mathbf{A}^{\mathrm{T}}\mathbf{A}=\begin{bmatrix}\mathbf{0} & \mathbf{0}\\ \mathbf{B} & \mathbf{0}\\ \mathbf{0} & \mathbf{0}\\ \mathbf{0} & \mathbf{B}\end{bmatrix}^{\mathrm{T}}\begin{bmatrix}\mathbf{0} & \mathbf{0}\\ \mathbf{B} & \mathbf{0}\\ \mathbf{0} & \mathbf{0}\\ \mathbf{0} & \mathbf{B}\end{bmatrix}=\begin{bmatrix}\mathbf{0} & \mathbf{B}^{\mathrm{T}} & \mathbf{0} & \mathbf{0}\\ \mathbf{0} & \mathbf{0} & \mathbf{0} & \mathbf{B}^{\mathrm{T}}\end{bmatrix}\begin{bmatrix}\mathbf{0} & \mathbf{0}\\ \mathbf{B} & \mathbf{0}\\ \mathbf{0} & \mathbf{0}\\ \mathbf{0} & \mathbf{B}\end{bmatrix}=\begin{bmatrix}\mathbf{B}^{\mathrm{T}}\mathbf{B} & \\ & \mathbf{B}^{\mathrm{T}}\mathbf{B}\end{bmatrix}. \tag{D2}$$

By substituting (6b) into (D2), we obtain

$$\begin{aligned}\mathbf{A}^{\mathrm{T}}\mathbf{A}&=\begin{bmatrix}\mathbf{V}_{\mathrm{B}}\boldsymbol{\Sigma}_{\mathrm{B}}^{\mathrm{T}}\mathbf{U}_{\mathrm{B}}^{\mathrm{T}}\mathbf{U}_{\mathrm{B}}\boldsymbol{\Sigma}_{\mathrm{B}}\mathbf{V}_{\mathrm{B}}^{\mathrm{T}} & \\ & \mathbf{V}_{\mathrm{B}}\boldsymbol{\Sigma}_{\mathrm{B}}^{\mathrm{T}}\mathbf{U}_{\mathrm{B}}^{\mathrm{T}}\mathbf{U}_{\mathrm{B}}\boldsymbol{\Sigma}_{\mathrm{B}}\mathbf{V}_{\mathrm{B}}^{\mathrm{T}}\end{bmatrix}\\ &=\begin{bmatrix}\mathbf{V}_{\mathrm{B}}\mathbf{Q}_{\mathrm{B}}^{2}\mathbf{V}_{\mathrm{B}}^{\mathrm{T}} & \\ & \mathbf{V}_{\mathrm{B}}\mathbf{Q}_{\mathrm{B}}^{2}\mathbf{V}_{\mathrm{B}}^{\mathrm{T}}\end{bmatrix}\\ &=\begin{bmatrix}\mathbf{V}_{\mathrm{B}}\mathbf{Q}_{\mathrm{B}}\mathbf{V}_{\mathrm{B}}^{\mathrm{T}} & \\ & \mathbf{V}_{\mathrm{B}}\mathbf{Q}_{\mathrm{B}}\mathbf{V}_{\mathrm{B}}^{\mathrm{T}}\end{bmatrix}^{2}.\end{aligned} \tag{D3}$$

With (D1)–(D3), we obtain

$$\mathbf{V}_{\mathrm{A}}\mathbf{Q}_{\mathrm{A}}^{2}\mathbf{V}_{\mathrm{A}}^{\mathrm{T}}=\begin{bmatrix}\mathbf{V}_{\mathrm{B}}\mathbf{Q}_{\mathrm{B}}\mathbf{V}_{\mathrm{B}}^{\mathrm{T}} & \\ & \mathbf{V}_{\mathrm{B}}\mathbf{Q}_{\mathrm{B}}\mathbf{V}_{\mathrm{B}}^{\mathrm{T}}\end{bmatrix}^{2}. \tag{D4}$$

By solving (D4), we obtain

$$\mathbf{V}_{\mathrm{A}}\mathbf{Q}_{\mathrm{A}}\mathbf{V}_{\mathrm{A}}^{\mathrm{T}}=\pm\begin{bmatrix}\mathbf{V}_{\mathrm{B}}\mathbf{Q}_{\mathrm{B}}\mathbf{V}_{\mathrm{B}}^{\mathrm{T}} & \\ & \mathbf{V}_{\mathrm{B}}\mathbf{Q}_{\mathrm{B}}\mathbf{V}_{\mathrm{B}}^{\mathrm{T}}\end{bmatrix}. \tag{D5}$$

We select the positive solution for simplicity as

$$\begin{aligned}\mathbf{V}_{\mathrm{A}}\mathbf{Q}_{\mathrm{A}}\mathbf{V}_{\mathrm{A}}^{\mathrm{T}}&=\begin{bmatrix}\mathbf{V}_{\mathrm{B}}\mathbf{Q}_{\mathrm{B}}\mathbf{V}_{\mathrm{B}}^{\mathrm{T}} & \\ & \mathbf{V}_{\mathrm{B}}\mathbf{Q}_{\mathrm{B}}\mathbf{V}_{\mathrm{B}}^{\mathrm{T}}\end{bmatrix}\\ &=\begin{bmatrix}\mathbf{V}_{\mathrm{B}} & \\ & \mathbf{V}_{\mathrm{B}}\end{bmatrix}\begin{bmatrix}\mathbf{Q}_{\mathrm{B}} & \\ & \mathbf{Q}_{\mathrm{B}}\end{bmatrix}\begin{bmatrix}\mathbf{V}_{\mathrm{B}} & \\ & \mathbf{V}_{\mathrm{B}}\end{bmatrix}^{\mathrm{T}}.\end{aligned} \tag{D6}$$

Let $\mathbf{V}_{\mathrm{A}}$ be

$$\mathbf{V}_{\mathrm{A}}=\begin{bmatrix}\mathbf{V}_{\mathrm{B}} & \\ & \mathbf{V}_{\mathrm{B}}\end{bmatrix}. \tag{D7}$$

From (D-6), we obtain

$$\mathbf{Q}_{\mathrm{A}}=\begin{bmatrix}\mathbf{Q}_{\mathrm{B}} & \\ & \mathbf{Q}_{\mathrm{B}}\end{bmatrix}. \tag{D8}$$

## APPENDIX E: ORTHOGONALITY OF $\mathbf{A_0}$

Self-projecting $\mathbf{A_0}$ becomes

$$\begin{aligned}\mathbf{A}_{o}^{\mathrm{T}}\mathbf{A}_{\mathrm{o}}&=\frac{1}{\sqrt{M}}\mathbf{A}_{\mathrm{o}}^{\mathrm{T}}\frac{1}{\sqrt{M}}\mathbf{A}_{\mathrm{o}}\\ &=\frac{1}{M}\left(\sum_{j=1}^{M}\boldsymbol{\Phi}_{j}\right)^{T}\sum_{i=1}^{M}\boldsymbol{\Phi}_{i}\\ &=\frac{1}{M}\sum_{i=1}^{M}\sum_{j=1}^{M}\boldsymbol{\Phi}_{j}^{\mathrm{T}}\boldsymbol{\Phi}_{i}.\end{aligned} \tag{E1}$$

By applying (A4) to (E1), we obtain

$$\begin{aligned}\mathbf{A}_{\mathrm{o}}^{\mathrm{T}}\mathbf{A}_{\mathrm{o}}&=\frac{1}{M}\sum_{i=1}^{M}\boldsymbol{\Phi}_{i}^{\mathrm{T}}\boldsymbol{\Phi}_{i}\\ &=\frac{1}{M}\sum_{i=1}^{M}\mathbf{I}\\ &=\mathbf{I}.\end{aligned} \tag{E2}$$